



# The development of small-molecule inhibitors targeting hexokinase 2

Wenyang Shan, Yan Zhou, Kin Yip Tam\*

Cancer Centre, Faculty of Health Sciences, University of Macau, Macau

As one of the well-known hallmarks of cancer malignancy, most proliferating cancer cells exhibit enhanced rates of glycolysis. Hexokinase 2 (HK2) is the rate-limiting enzyme catalyzing the first step of glycolysis, and is often overexpressed in most cancer cells. Thus, targeting HK2 appears to be a promising anticancer therapy. However, selective inhibition of HK2 and the polar nature of the target site remain challenges to the development of small-molecule inhibitors, which could be addressed by targeting unique domains of HK2, such as its N-terminal domain. Here, we review different target-inhibitor binding modes and the associated pharmacological effects, which would be informative for rational molecular design. We also highlight further perspectives and strategies to develop novel HK2 inhibitors for cancer therapy.

**Keywords:** Cancer metabolism; Hexokinase 2; Drug-target binding; Selective inhibition; Structure-based molecular design

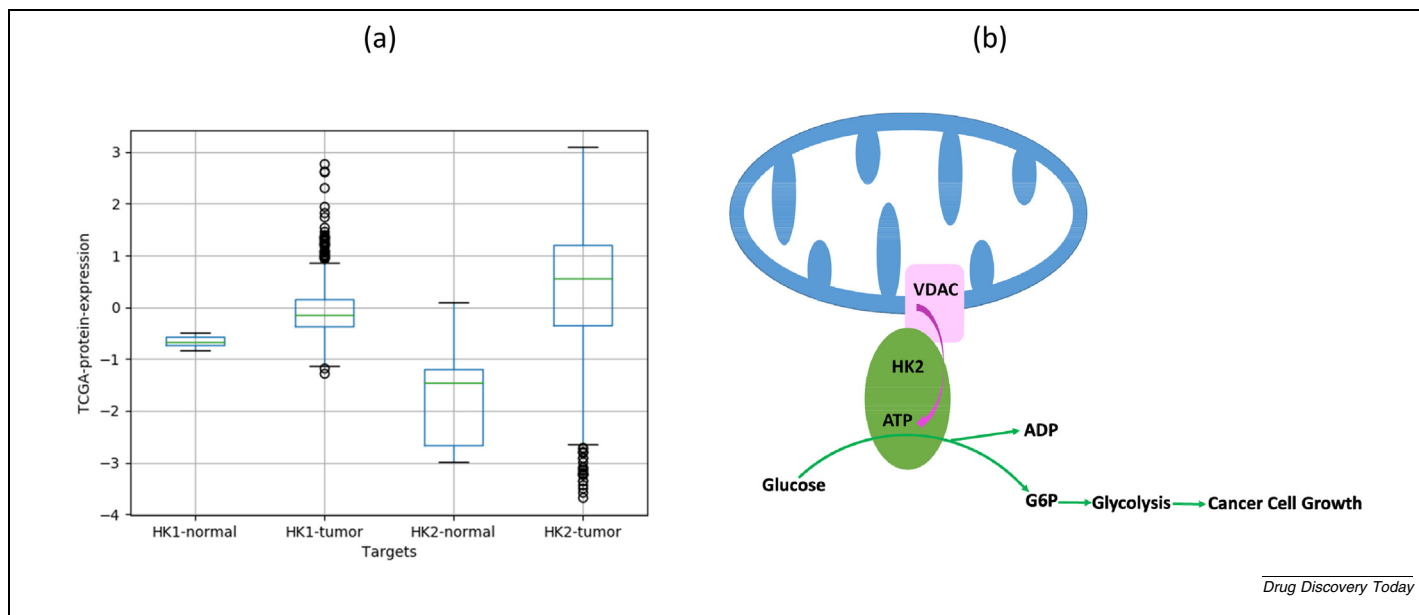
## Introduction

Proliferative cancer cells often exhibit an enhanced rate of glycolysis, known as the Warburg effect.<sup>1–3</sup> In contrast to normal cells, in which glucose metabolism is typically undertaken via mitochondrial oxidative phosphorylation (OXPHOS), most cancer cells benefit from enhanced glycolysis by rapidly generating ATP and precursors for building biomass.<sup>4</sup> The dependence on glycolysis facilitates the growth of cancer cells. Thus, targeting cancer metabolism could be a promising anticancer strategy. However, only a limited number of anticancer drugs tackling cancer metabolism have been approved.<sup>5</sup>

HK, a rate-limiting enzyme responsible for the first irreversible step of glycolysis, catalyzes glucose to glucose-6-phosphate (G6P). It is also implicated in other pathways, such as the tricarboxylic acid cycle, the pentose phosphate pathway, and the synthesis of nucleotides, lipids, as well as amino acids that are required for rapid cancer growth.<sup>2,6,7</sup> Currently, five human HK isoenzymes have been identified, namely HK1, HK2, HK3, HK4,

and the newly discovered hexokinase domain-containing protein 1 (HKDC1).<sup>8</sup> Among these isoforms, HK1-3 and HKDC1 are 100-kDa proteins, whereas HK4 is half the size of other isoenzymes with only a single domain of much lower affinity for the glucose substrate.<sup>9–13</sup> The retention of the HK function and enzyme activity of HKDC1 have not yet been fully characterized.<sup>8</sup> HK3 is a weakly expressed isozyme in mammalian cells,<sup>14</sup> whereas HK1 is the main isoenzyme ubiquitously expressed in all mammalian tissues.<sup>11</sup> HK2 is the major isoenzyme overexpressed in various types of cancer,<sup>7,15–18</sup> suggesting a key role in reprogrammed glucose metabolism in cancer cells. To corroborate the importance of HK in cancers, we explored the HK1 and HK2 expression data in The Cancer Genome Atlas (TCGA) database (<https://portal.gdc.cancer.gov>), from which 867 tumor samples and seven normal samples were collected. Protein expression quantification data were downloaded and analyzed in Python 3.7. HK2 is overexpressed in tumor samples compared with HK1 (Fig. 1a), while HK1 is the major isoenzyme in normal

\* Corresponding author. Tam, K.Y. ([kintam@um.edu.mo](mailto:kintam@um.edu.mo))

**FIGURE 1**

Targeting hexokinase 2 (HK2) for anticancer therapy. **(a)** Comparison of HK1 and HK2 expression in normal and tumor samples archived in The Cancer Genome Atlas (TCGA) database. The Y-axis represents the protein expression levels obtained from the TCGA database. **(b)** Schematic of HK2 binding with VDAC1 to maintain cancer cell growth. HK2 binds to the VDAC1 at the outer mitochondria membrane enabling the preferential transport of ATPs from mitochondria to cytosol, which are then utilized by the HK enzymes to facilitate glycolysis.

samples compared with HK2. Thus, its overexpression in cancer cells and its relevance to glycolysis render HK2 an attractive anti-cancer target.

Voltage-dependent anion channels (VDAC) are gatekeepers for the transport of mitochondrial metabolites, including adenine nucleotides, ATP, and ions across the outer mitochondrial membrane (OMM).<sup>19</sup> VDAC1 is the major anion channel form at the OMM and is often overexpressed in many types of cancer.<sup>20</sup> HK2 was found to bind to VDAC1 at the OMM (Fig. 1b), resulting in the preferential transport of ATP from mitochondria to the cytosol, which was then used by HKs to facilitate glycolysis. Moreover, the association of HK2 with VDAC1 protected cancer cells from apoptosis.<sup>21–23</sup> VDAC1 itself has been shown to promote mitochondrial-mediated apoptosis by binding to the proapoptotic protein, B cell lymphoma-2-associated X (Bax), followed by cytochrome c release and caspase cascade initiation. By binding to VDAC1 and competing with Bax, HK2 effectively interferes with key apoptotic pathways, thereby helping cancer cells escape their apoptotic fate.<sup>24</sup> Therefore, inhibiting the interaction between HK2 and VDAC1 could provide another strategy for cancer therapy. However, the crystal structure of the HK2–VDAC1 complex is currently unavailable, which hampers the molecular design of inhibitors targeting this interaction.

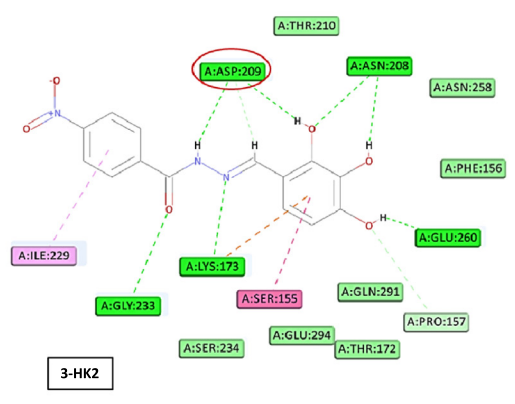
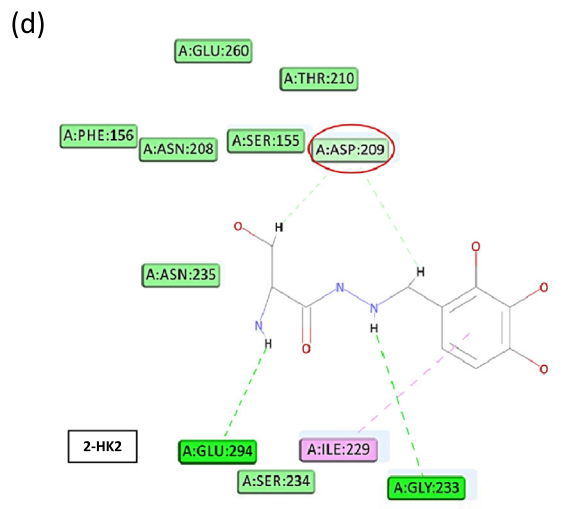
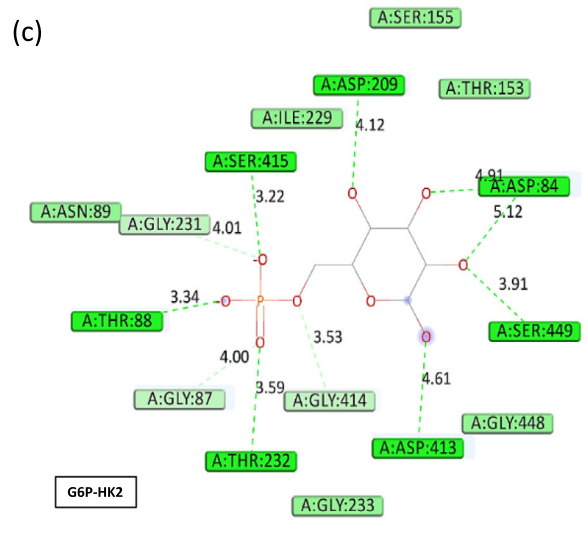
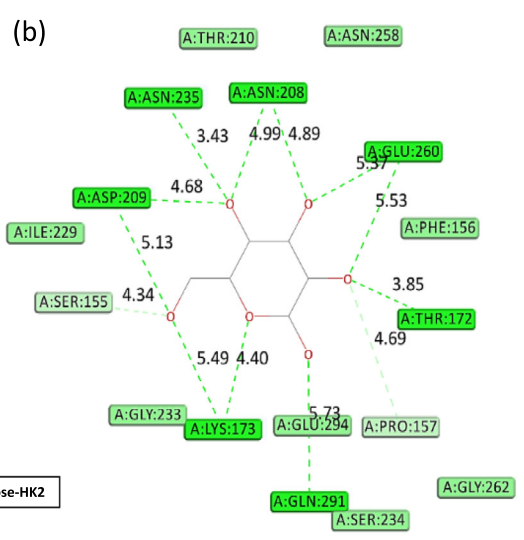
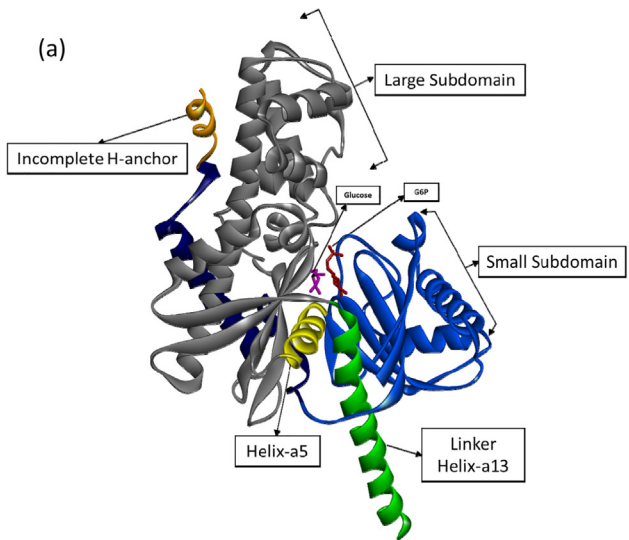
Attempts have been made to design small-molecule inhibitors of HK2, but the polar nature of the active site and the selective inhibition of the specific isoenzyme remain some of the challenges to developing novel inhibitors.<sup>25–28</sup> Human HK1–3 contain N- and C-terminal domains that are equal in size and structurally similar, and each domain contains a conserved glucose-binding pocket.<sup>29</sup> However, HK2 has catalytic functions in both the N- and C-terminal domains, whereas HK1 and HK3

only have catalytic functions in the C-terminal domain. Thus, targeting the N-terminal domain could be an important avenue for designing selective HK2 inhibitors.<sup>9,10,29–31</sup> Recently, three specific residues responsible for maintaining the N-terminal catalytic function of HK2 in the linker helix- $\alpha$ 13 were confirmed experimentally: ASP447, SER449, and LYS451.<sup>32</sup>

In this review, we summarize the structural information of HK2 available, including the glucose and G6P-binding domains and the active site of HK2 catalytic function. In addition to these commonly investigated domains, we highlight the unique linker in the N-terminal domain, which specifically maintains the catalytic function of HK2. We also review some of the known HK2 inhibitors and their binding modes with the target protein. To rationalize binding modes with the HK2–VDAC1 complex, we constructed a homology model of the target, enabling the identification of key molecular interactions between the inhibitors and the complex. Only a limited number of HK2 inhibitors have been reported so far. Some of these original hit molecules were discovered from high-throughput screening or virtual screening, whereas others were derived from natural products. We hope that this review will renew interest in the structure-based molecular design of potent and selective HK2 inhibitors.

### Structure of HK2

Several crystal structures of HK2 are available in the Protein Data Bank (PDB), among which only one study reported the original structure of HK2 (PDB ID: 2NZT), whereas others are co-crystallized with other small-molecule inhibitors (PDB ID: 5HEX, 5HFU, and 5HG1) and cannot represent the native state of HK2. Thus, the crystal structure of human HK2 (PDB ID: 2NZT, resolution: 2.45 Å) was used in the present study. The



(e)

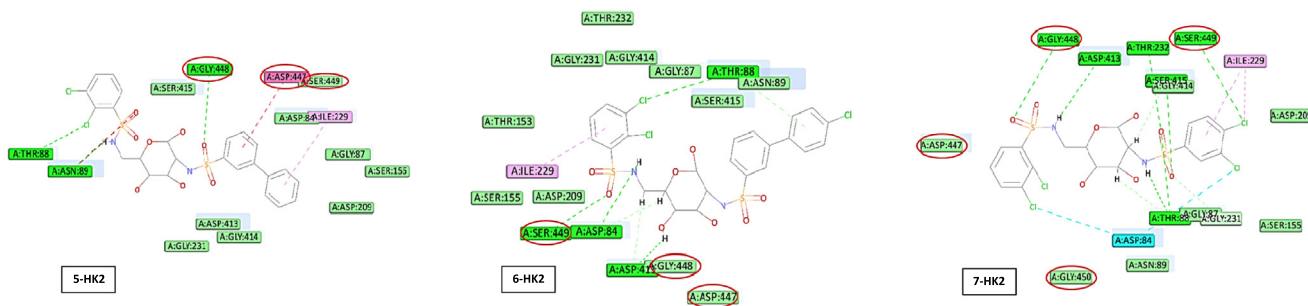


Fig. 2 (continued)

N-terminal half of HK2, including the unique linker responsible for the activity of HK2, was selected for illustration because of the highly conserved structure of the C-terminal half, as seen in other HK isoenzymes.

Fig. 2a depicts the structure of HK2, together with glucose and G6P binding to its N-terminal domain. The interactions between glucose and G6P with HK2 are shown in Fig. 2b,c, respectively. All polar interactions are predominant, suggesting the polar nature of the catalytic domain of HK2. Glucose locates near the catalytic helix-a5, which is responsible for catalyzing glucose to G6P. Inhibitors designed to target the glucose-binding domain could compete with the binding of glucose to HK2. Moreover, G6P, as the product of glucose catalyzed by HK2, is a natural inhibitor of HK2. However, the inhibitory mechanism of G6P is not fully understood.<sup>33</sup> From the location of G6P in HK2 in Fig. 2a (situated near the helix-a5 and helix-a13 domains) and the interactions of G6P with HK2 in Fig. 2b, it can be seen that G6P could be competing with glucose binding and might disrupt the unique catalytic structure of HK2 to exert a selective inhibitory function. The incomplete H-anchor (orange) in the N-terminal half of HK2 (Fig. 2a) is discussed below.

### Inhibitors targeting the glucose-binding site

Inhibitors competing with glucose had been developed for some time. 2-Deoxy-D-glucose (**1**, 2DG) was the earliest inhibitor, first developed during the 1950 s.<sup>34</sup> It was reported that 10.0 mM of **1**

can inhibit the expression of HK2 in HeLa cells.<sup>35</sup> However, **1** exhibited adverse effects in the clinic, resulting in trials being discontinued.<sup>36</sup> Over recent decades, virtual screening has offered the exciting possibility to identify novel HK2 inhibitors with new pharmacophores/scaffolds. For instance, benserazide (**2**, Benz)<sup>26</sup> and benitrobenrazide (**3**, BNBZ)<sup>27</sup> were developed by virtual screening to specifically target the glucose-binding site in HK2. Inspired by **2**, **3** was subsequently developed, which exhibited more-potent inhibition against HK2. However these studies did not consider the design of inhibitors in terms of their drug-target binding modes. Information about inhibitors targeting the glucose-binding site, including their structures, binding affinities, enzyme inhibition activities, and IC<sub>50</sub>s for cell viability inhibition in different cell lines, are summarized in Table 1.

Targeting the glucose-binding pocket would be useful to aid *in silico* molecular design. Fig. 2d shows the molecular interactions of **2** and **3** with the glucose-binding pocket of HK2. Compared with **2**, **3** was modified through the introduction of a phenyl ring and aromatization of one of the hydrazine nitrogens, which enhanced its nonpolar and polar interactions with the binding pocket, respectively. This might be one reason why **3** was tenfold more potent against HK2 compared with **2**.

### Inhibitors mimicking G6P binding

Early studies reported that metformin (**4**) exhibited HK2 enzymatic inhibitory effects at mM concentrations similar to G6P

## FIGURE 2

Structure depictions of hexokinase 2 (HK2) and the binding modes of inhibitors targeting the glucose- and glucose-6-phosphate (G6P)-binding sites. (a) Crystal structure of the N-terminal half of HK2. The N-terminal half of HK2 comprises two subdomains: large subdomain (ASN208-ASP447, blue) and small subdomain (ASP73-VAL207, gray). The helix-a5 (residues: ASP209-ASP220, yellow) linking these two subdomains has a catalytic function. Specifically, the residue ASP209 in the helix-a5 is responsible for the catalytic function in the N-terminal domain. The linker helix-a13 (residues GLY447-GLN478, green), which links the N- and C-terminal halves of HK2, together with helix-a5, maintains the unique catalytic structure of the N terminus. Glucose and G6P are overlaid at their corresponding binding sites. (b) Interactions between HK2 and glucose. Glucose interacts with ASP209 of HK2 via two hydrogen bond interactions. (c) Interactions between HK2 and G6P. G6P interacts with ASP209 of HK2 via one hydrogen bond interaction. G6P interacts with the SER449 residue in the linker helix-a13, which is responsible for the unique catalytic structure of HK2, via strong hydrogen bond interactions. (d) Interactions of **2** and **3** with the HK2 glucose-binding pocket. Polar interactions between ligand and target are dominant, in which **2** and **3** pick up two and three hydrogen bond interactions with ASP209, respectively. (e) Interactions of **5–7** with the HK2 G6P-binding pocket. **5–7** all interact with three residues (ASP447, GLY448 and SER449), which reside in the linker helix-a13 to maintain the unique catalytic function of N-terminal of HK2.<sup>32</sup> **7** picks up an additional interaction with GLY450, which is situated in linker helix-a13, in close proximity to another key residue, LYS451, which is crucial for the unique catalytic function. Graphics generated using Discovery Studio 2016. Light green indicates van der Waals, dark green indicates conventional hydrogen bonds, light green indicates carbon hydrogen bond, light purple indicates alkyl and Pi-alkyl, turquoise indicates halogen (Cl, Br, I), light green indicates Pi-donor hydrogen bond, pink indicates amide-Pi stacked.

TABLE 1

## Summary of available HK2 inhibitors and their enzymatic and cell activity data.

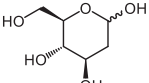
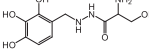
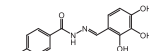
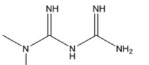
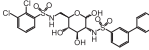
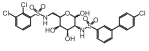
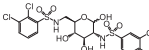
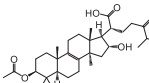
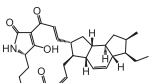
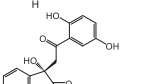
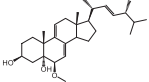
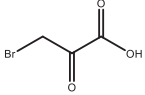
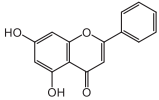
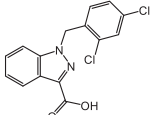
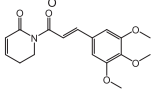
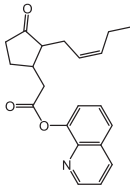
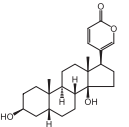
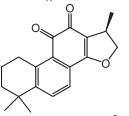
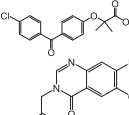
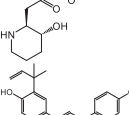
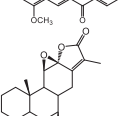
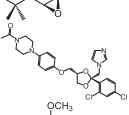
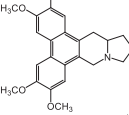
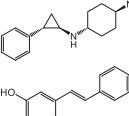
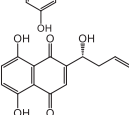
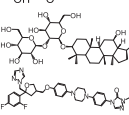


Inhibitor ID	Chemical structure	Inhibitor–protein binding mode	IC <sub>50</sub> for HK inhibition	K <sub>d</sub> for HK2	IC <sub>50</sub> for cell viability inhibition	IC <sub>50</sub> for HK2–VDAC1 inhibition	Enzyme source	Enzyme inhibition (experimental conditions)	Activities for HK2–VDAC1 inhibition in cell lines	Cellular HK2–VDAC1 inhibition (experimental conditions)	Refs
1		Targets glucose-binding site	N/A								34
2			5.5 μM for HK2; 25.0 μM for HK1	149.0 μM	143.0 μM for SW480	N/A	Recombinant HK2	85 μL assay mix containing 100 mM Tris HCl pH 8.0, 5 mM MgCl <sub>2</sub> , 200 mM glucose, 0.8 mM ATP, 1 mM NAD <sup>+</sup> , 0.25 units of G6P-DH, enzyme inhibition calculated based on changes in absorbance of NADH at 340 nm. 85 μL assay for 2 and 70 μL assay for 3	N/A		26
3			0.5 μM for HK2; 2.2 μM for HK1	5.0 μM	24.0 μM for SW1990; 7.1 μM for SW480	N/A			N/A		27
4		Mimics G6P binding and targets HK2–VDAC1 binding	N/A								37
5		Mimics G6P binding	25.0 nM for HK2; 5.0 μM for HK1	N/A			Kit produced by Promega	Using 1 nM enzyme, ATP, citrate, and glucose concentrations were 100 μM, 1 mM, and 100 μM, respectively; all reactions carried out in 100 mM Hepes buffer, pH 7.2 containing 0.1 M KCl, 10 mM MgCl <sub>2</sub> , 2 mM dithiothreitol, 0.05 mgN/AmL BSA, and 0.05% CHAPS detergent; procedure quantified amount of MgADP generated from HK reaction in presence of MgATP and glucose through UV absorbance at 613 nm	N/A		25
6			7.9 nM for HK2; 1.0 μM for HK1	N/A					N/A		
7			50.0 nM for HK2; >20.0 μM for HK1	N/A					N/A		
8		Mimics G6P binding and targets HK2–VDAC1 binding	5.0 μM for HK2	N/A			Cell lysates	100 mM Tris HCl (pH 8.0), 5 mM MgCl <sub>2</sub> , 100 mM glucose, 0.8 mM ATP, 1 mM NADP, and 3 units G6P dehydrogenase. NADP reduction in UV absorbance at 340 nm was monitored	10.0–100.0 μM in SK-BR-3 cells	After treatment with 8, dose-dependent mitochondrial HK2 dissociation observed. Dissociation of HK2 and VDAC1 induced release of mitochondrial Cyt c, resulting from treatment with 8	38
9		Mimics G6P binding	No IC <sub>50</sub> values but compared with other inhibitors	4.1 μM	1.3 μM for PANC-1	N/A	Protein HK2 (BioVision)	HK colorimetric assay kit (Biovision)	N/A		39
10			17.5 μM for HK2	N/A	62.1 μM for HeLa; 62.5 μM for HepG2; 54.6 μM for A549	N/A	HK activity assay kit (Abcam)	HK activity assay kit (Abcam)	N/A		28
11			2.1 μM for HK2	114.5 μM	5.1 μM for SW1990; 22.6 μM for Vero	N/A	Recombinant HK2	10 μL recombinant HK2 (100 nM) incubated with 5 μL inhibitor at 37 °C for 10 min; 85 μL assay mix containing 100 mM Tris HCl pH 8.0, 5 mM MgCl <sub>2</sub> , 200 mM glucose, 0.8 mM ATP, 1 mM NAD <sup>+</sup> , 0.25 units of G6P-DH, added;	N/A		40

TABLE 1 (CONTINUED)

Inhibitor ID	Chemical structure	Inhibitor-protein binding mode	IC <sub>50</sub> for HK inhibition	K <sub>d</sub> for HK2	IC <sub>50</sub> for cell viability inhibition	IC <sub>50</sub> for HK2-VDAC1 inhibition	Enzyme source	Enzyme inhibition (experimental conditions)	Activities for HK2-VDAC1 inhibition in cell lines	Cellular HK2-VDAC1 inhibition (experimental conditions)	Refs
12		Targets HK2-VDAC1 binding	N/A					enzyme inhibition IC <sub>50</sub> values for inhibitor calculated based on changes in NADH at fluorescence (Ex340N/AEm460 nm)	100.0 μM in HL-60 cells	Mitochondria isolated from HL-60 cells resuspended in buffer containing KCl, and incubated with clotrimazole (CTZ), G6P, or 12 to test direct effect of these compounds. CTZ dissociates HK2 from mitochondria by targeting interaction of HK2 and VDAC1, whereas G6P inhibits HK. 12 not only caused upshift in HK2, but also led to release of HK2 from mitochondria	48
13			N/A						30.0 μM in HCC-LM3 cells	HK2 in mitochondria substantially decreased in dose-dependent manner after exposure to 13, with reduction of HK2 in mitochondria, HK2 bound to VDAC1 also significantly decreased. Cleaved caspase-3 and PARP, markers indicating cell apoptosis, were dramatically elevated, suggesting that decrease in HK2 and disruption of HK2N/AVDAC1 interaction caused by 13 resulted in cancer cell apoptosis	49
14			N/A								50
15			N/A						5.0 μM in HCC827 and H1975 cells	Phosphorylation of HK2 on Thr473 is required for its localization on mitochondria. HK2 phosphorylation in HCC827 cells was determined: 15 significantly suppressed Thr473 phosphorylation in a dose-dependent manner and promoted activation of intrinsic apoptosis signaling pathway, including release of cytochrome c and Bax translocation to mitochondria	51
16			N/A			92.0 nM	Human HK1 and HK2 plasmids (Addgene) purified from <i>Escherichia coli</i> . VDAC1 purified from sheep liver mitochondria	HKs pre-incubated with VDAC1 for 10 min; increasing concentrations of 16 added for additional 10 min. All studies were done at room temperature in assay buffer of 20 mM Tris, 10 mM glucose, 10 mM MgCl <sub>2</sub> , and 1% DMSO at pH 7.5	IC <sub>50</sub> in human skin SCC A431 cells: ~0.8 μM	Cellular effect of 16 demonstrated in human skin SCC A431 cells (which expressed both HK1 and HK2). Semiquantification of western blot revealed dose-dependent reduction in mitochondrial-bound HK2 levels, with IC <sub>50</sub> of ~ 0.8 μM. This occurred without changes in total cellular HK2 levels, suggesting direct effect on binding of HK2 to mitochondria. 16 reduced cellular ATP levels by ~ 50% after 2-h incubation in A431 cells, demonstrating energetic outcome of HK2 dissociation from mitochondria. 16 treatment resulted in apoptosis induction, demonstrated by reduction in cytochrome C levels in	52,53

(continued on next page)

TABLE 1 (CONTINUED)

Inhibitor ID	Chemical structure	Inhibitor-protein binding mode	IC <sub>50</sub> for HK inhibition	K <sub>d</sub> for HK2	IC <sub>50</sub> for cell viability inhibition	IC <sub>50</sub> for HK2-VDAC1 inhibition	Enzyme source	Enzyme inhibition (experimental conditions)	Activities for HK2-VDAC1 inhibition in cell lines	Cellular HK2-VDAC1 inhibition (experimental conditions)	Refs
17		Unknown	N/A		21.5 nM for A2780; 25.6 nM for Hey	N/A				mitochondrial fraction within 2 h of treatment and increase in cellular levels of cleaved caspase-3 within 6 h of treatment	56
18			N/A		11.2 μM for A2780; 18.4 μM for Hey	N/A					57
19			N/A			N/A					58
20			N/A		5.8 nM for HCT116	N/A					59
21			N/A		55.6 mM for SGC7901	N/A					60
22			N/A		60.8 μM for H1299	N/A					61
23			N/A		8.0–10.0 mM (EC <sub>50</sub> ) for GBM	N/A					62
24			N/A			N/A					63
25			N/A		61.0 μM for A549	N/A					64
26			N/A		59.5 μM for HCC-LM3	N/A					65
27			N/A		19.9 mM for Eca109	N/A					66
28			N/A		59.0 μgN/A mL for A2780	N/A					67
29			N/A		8.0–10.0 mM (EC <sub>50</sub> ) for GBM	N/A					62

mimics.<sup>37</sup> Recently, **5–7** were designed as G6P mimics that exhibited good HK2 inhibitory potency and selectivity.<sup>25</sup> However, no further investigation was conducted on the link between mimicking G6P binding and selective inhibition in terms of the drug–target binding modes. In the same study, the crystal-protein structures of three other less-potent HK2 inhibitors were reported (PDB ID: 5HEX, 5HFU, and 5HG1), which provided useful information for the *in silico* molecular design of G6P mimics.<sup>25</sup> Pachymic acid (**8**, PA) is a natural product that was reported as a HK2 inhibitor. Molecular docking suggested that **8** could be a G6P mimic.<sup>38</sup> Ikarugamycin (**9**) was reported to be a HK2 inhibitor. A docking study was used to corroborate the binding of **9** with HK2 (PDB ID: 5HFU).<sup>39</sup> LY2019-001 (**10**) was a patented molecule derived from virtual screening against the binding pocket of HK2 (PDB ID: 5HEX).<sup>28</sup> **11**, a steroid from *Ganoderma sinense*, exhibited HK2 inhibition function.<sup>40</sup>

To study the binding modes of **5–7** and investigate the relationship between mimicking G6P binding and selectivity, we conducted docking to the G6P-binding site and visualized the molecular interactions. As shown in Fig. 2e, **5–7** all interacted with three common residues (ASP447, GLY448, and SER449) residing in the linker helix- $\alpha$ 13 to maintain the unique catalytic function of the N terminus of HK2, whereas **7** picked up an additional interaction with residue (GLY450), which is critical for the unique catalytic function of HK2,<sup>32</sup> suggesting itself to be the most-selective HK2 inhibitor among these three molecules.

We also sought to derive key active fragments that were likely to interact with the G6P-binding site. G6P has two key fragments that bind to HK2, namely, the glucose fragment and the phosphoric acid fragment. For inhibitors mimicking G6P binding, key fragments could be designed to mimic the G6P fragments. Indeed, **5–7** were designed with these notions in mind, namely a sulfonamide fragment that mimics the phosphate fragment and a polyhydroxy-pyran fragment that mimics the glucose fragment. These fragments can form strong hydrogen bond interactions with the G6P-binding site. In addition to fragments specifically designed to mimic G6P fragments, other inhibitors derived from other studies also have similar key fragments. For instance, **8** and **11** are both natural products and have a cyclopentane phenanthrene fragment in common. In addition to the polycyclic fragments to enable occupancy of the G6P-binding site, these two inhibitors also have hydroxyl, ester, ether, carboxyl, and other polar fragments that can form hydrogen bonds with the G6P-binding site. Moreover, the lactam heterocycle fragments in **9** and **10** are able to form hydrogen bond interactions with the target. However, molecules with high polarity could hamper permeation through various biological barriers, which could lead to suboptimal target engagement, high renal clearance (short *in vivo* half-life), and poor bioavailability. Therefore, it is important to optimize the permeability and lipophilicity of the molecules, while maximizing the nonpolar and polar interactions with the binding pocket. With regard to **5–7**, all three compounds have phenyl rings, which can form pi-alkyl nonpolar interactions with the alkyl fragment of residue ILE229. In addition, the phenyl rings of **5** can form amide-pi stacked nonpolar interactions with the amino group of ASP447, which could be responsible for the selective inhibition of HK2. Hence, nonpolar fragments, such as phenyl and

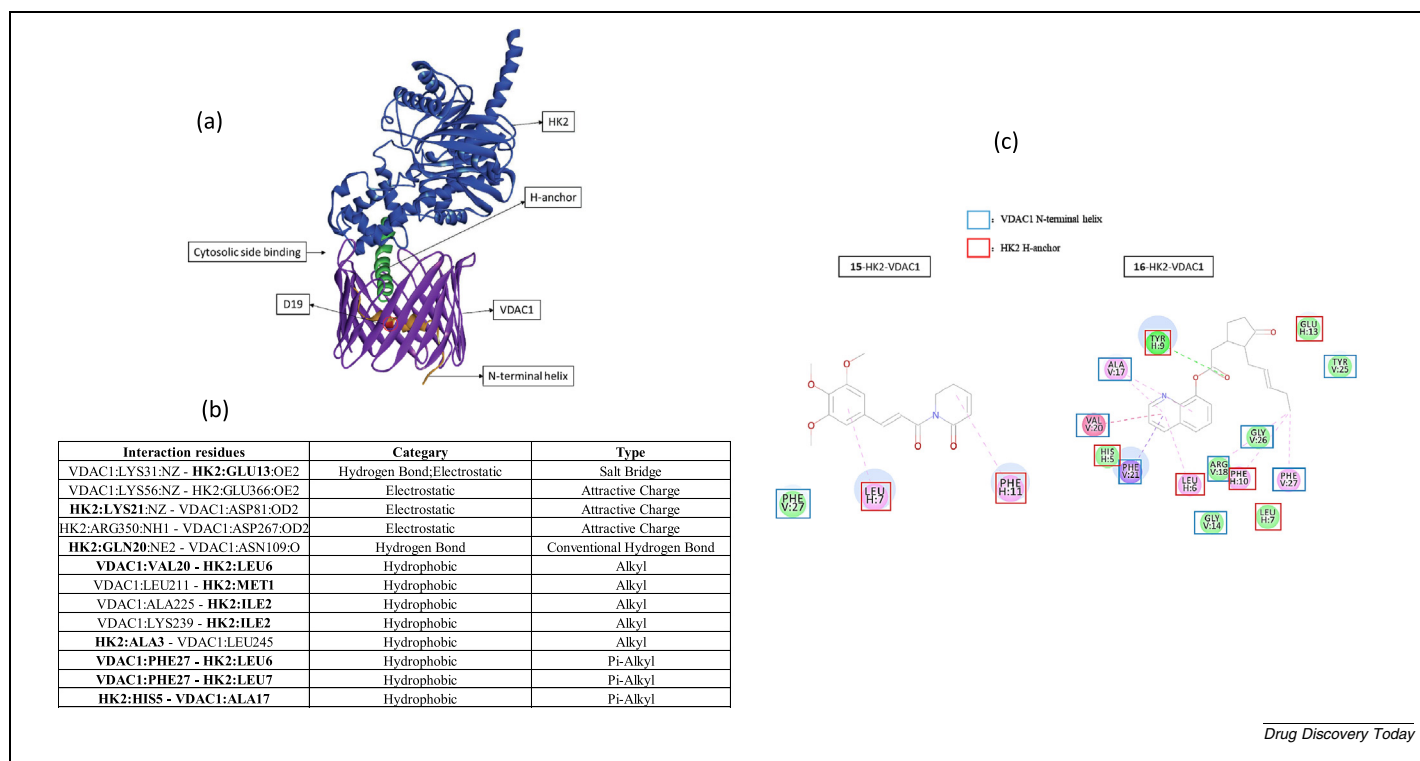
cycloalkyl, are useful to reduce the polarity of the molecule, which would enhance its lipophilicity and permeability. Thus, these fragments, together with their bioisosteres, are worth considering for the further molecular design of HK2 inhibitors mimicking G6P binding.

### Inhibitors targeting HK2–VDAC1 binding

HK1,2 were reported to bind with the membrane of mitochondria through the short N-terminal hydrophobic helix (H-anchor) (residues 1–27) more specifically, which was responsible for the interaction with mitochondria.<sup>41–46</sup> Further study revealed that the binding of HK2 with VDAC1 could free Asp19 to restrict the movement of the N-terminal helix of VDAC1 responsible for the interaction with HK2.<sup>47</sup> The complete structure of the H-anchor of HK2 is not available, because the incomplete H-anchor lacks residues 1–16, which is an obstacle for the construction of the HK2–VDAC1 complex (Fig. 2a). To address this problem, attempts have been made to construct a homology HK2 model by using the highly homologous isoform from rat, HK1 (PDB ID: 1BG3, resolution: 2.80 Å) as a template. The H anchor of rat HK1 shares high sequence similarity with human HK2, which enabled the description of the dynamic process of HK2 binding to the mitochondria membrane and showed how VDAC1 phosphorylation disrupts HK2 binding. However, less information is available on the interactions of residues between HK2 and VDAC1, which might render this model incomplete for use in *in silico* HK2 inhibitor design.<sup>42</sup> Another HK2–VDAC1 binding model was also constructed using the incomplete H-anchor of HK2 (PDB ID: 2NZT).<sup>47</sup> Here, we constructed a homology model of the HK2–VDAC1 complex, which was established according to the crystal structure of HK1 (PDB ID: 1BG3, resolution: 2.80 Å) to complete the incomplete structure of the H anchor of HK2, through a homology modeling web-tool (Swiss Models; [expasy.org](http://expasy.org)). The structure of VDAC1 (PDB ID: 2JK4, resolution: 4.10 Å) was used to dock with HK2. According to the key residues of HK2 and VDAC1 mentioned above, which are responsible for the interactions, we further conducted protein–protein docking through the web tool ZDOCK (<https://zdock.umassmed.edu/>). The HK2–VDAC1 binding complex is shown in Fig. 3a, whereas the interactions of HK2 with VDAC1 are shown in Fig. 3b. Asp19 of the N-terminal helix of VDAC1 is not included in the interaction with H anchor of HK2, which is in line with a previous report.<sup>47</sup>

To date, inhibitors targeting HK2–VDAC1 binding were all discovered through screening of pharmacologically active compounds. Besides targeting G6P binding, **4** has also been reported to bind to the HK2–VDAC1 complex at mM concentrations.<sup>37</sup> Other than mimicking the G6P-binding mechanism as mentioned above, **8** was found to inhibit HK2–VDAC1 binding.<sup>38</sup> Moreover, 3-bromopyruvate (**12**, 3-BP) was reported to inhibit the interaction of HK2 with VDAC1.<sup>48</sup> Chrysin (**13**), a natural product, can also inhibit the interaction of HK2 with VDAC1.<sup>49</sup> Lonidamine (**14**), which is known to affect cancer cell proliferation, has been reported to inhibit HK2–VDAC1 binding.<sup>50</sup> Piperlongumine (**15**), a natural product, was reported to inhibit the interaction between HK2 and VDAC1,<sup>51</sup> whereas **16** selectively dissociated HK2 from VDAC1 at both the enzymatic and cellular



**FIGURE 3**

Structure of the hexokinase 2-voltage-dependent anion channel 1 (HK2-VDAC1) complex and the binding modes of inhibitors targeting the HK2-VDAC1 interaction. **(a)** Homology model of HK2-VDAC1 complex. Homology HK2 (blue) was successfully docked into the channel of VDAC1 (purple) through interactions between the H anchor (green) of HK2 and the N-terminal helix (orange) of VDAC1, while HK2 inhibitor binding to VDAC1 occurred on the cytosolic side. **(b)** Interactions between HK2 and VDAC1. HK2 interacts with VDAC1 with many nonbond interactions, including hydrogen bonds, and electrostatic and hydrophobic interactions. The residues involved in the interactions include residues (black bold) in the H anchor of HK2 and the N-terminal helix of VDAC1. **(c)** Interactions of **15** and **16** with the HK2-VDAC1 complex. **16** forms more interactions with residues crucial for HK2-VDAC1 binding than does **15**. Graphics were generated using Discovery Studio 2016. Blue outline indicates residues in VDAC1 N-terminal helix, red outline indicates residues in HK2 H anchor; light green indicates van der Waals, dark green indicates conventional hydrogen bonds, dark purple indicates Pi-sigma, pink indicates amide-Pi stacked, light purple indicates alkyl and Pi-alkyl.

levels.<sup>52,53</sup> Information about the inhibitors targeting HK2-VDAC1 binding, including the structures, enzyme inhibition activities, and cellular HK2-VDAC1 inhibition activities, are summarized in Table 1.

Of the above inhibitors targeting HK2-VDAC1 binding, only **15**<sup>51</sup> and **16**<sup>52,53</sup> were potent enough to warrant further analysis. To this end, we docked these two potent inhibitors to the homology HK2-VDAC1 binding complex (Fig. 3a): **16** made more interactions with residues crucial for HK2-VDAC1 binding than did **15** (Fig. 3c) This observation not only corroborates the more potent inhibitory effect of **16**, but also demonstrates the rationality of our homology HK2-VDAC1 model, suggesting it could offer useful information for *in silico* molecular design to target HK2-VDAC1 binding. Although the binding modes of **15** and **16** with our homology HK2-VDAC1 model were identified, molecular dynamics simulation should be performed to further corroborate our observations.

Although disrupting HK2-VDAC1 binding could facilitate cancer cell apoptosis, it might introduce cardiovascular safety liabilities (and/or probably other organs), because HK-VDAC1 binding appears to be vital for normal functioning of the heart.<sup>46,54,55</sup> Therefore, particular attention should be paid to the toxicological evaluation of such inhibitors. Interestingly, it was reported that, in rat cardiac muscle fibers, G6P binding alone

was not enough to induce detachment of HK2 from mitochondria, whereas lowering the intracellular pH to 6.3 was a necessary condition to induce detachment.<sup>55</sup> This suggests that intracellular pH is an important factor in attaching/detaching HK2 to mitochondria. It was hypothesized that the binding of HK2 to the mitochondria might involve histidine residues, which, in low pH, become positivity charged, facilitating dissociation.<sup>55</sup> The involvement of histidine in the HK2-VDAC1 binding was identified in our homology model (Fig. 3b) and the binding of **16** with HK2-VDAC1 (Fig. 3c).

### Other inhibitors with unknown drug-target binding modes

The binding modes of other HK2 inhibitors (**17-29**), downregulating HK2 expression levels and/or exhibiting inhibitory effects against HK2, were not confirmed in the original references, but require further investigation. Most of these were derived from natural products. For instance, bufalin (**17**),<sup>56</sup> cryptotanshinone (**18**),<sup>57</sup> fenofibrate (**19**),<sup>58</sup> halofuginone (**20**),<sup>59</sup> licochalcone A (**21**),<sup>60</sup> jolkinolide B (**22**),<sup>61</sup> ORY-1001 (**25**)<sup>64</sup>, the natural product resveratrol (**26**),<sup>65</sup> and ginsenoside 20(S)-Rg3 (**28**)<sup>67</sup> were reported to inhibit cell viability and HK2 expression *in vitro*. Ketoconazole (**23**)<sup>62</sup> and posaconazole (**29**)<sup>62</sup> exhibited inhibi-

tion of cell viability and inhibition of HK2 expression *in vivo*, while NK007 (**24**) increased HK2 protein degradation at 100.0 nM in A2780 cells and<sup>63</sup> shikonin (**27**) exhibited inhibition of cell viability.<sup>66</sup> The information relating to these inhibitors with unknown binding modes, including their structures and IC<sub>50</sub> values for cell viability inhibition in different cell lines, is summarized in Table 1.

With the exception of **28** and **29**, these inhibitors were successfully docked into the G6P-binding site (but failed to dock into the glucose-binding site). However, further experiments and structural studies are required to confirm whether HK2 is the target of these inhibitors and to elucidate the inhibitory mechanisms involved. Nevertheless, virtual screening against the G6P-binding pocket might be helpful to identify potentially active hit molecules from diverse compound libraries and/or natural product databases, which could open numerous opportunity to develop novel scaffolds from these hits.

### Concluding remarks

According to the structure of HK2, it should be possible to design inhibitors to target the glucose-binding site, the G6P-binding site, the linker helix-a13, which maintains the unique catalytic function of the N-terminal half of HK2, and the interaction domain of the HK2–VDAC1 complex.

To design inhibitors targeting the glucose-binding site, the residue ASP209 in the helix-a5 is the key target (N-terminal half of HK2 as an example). Additional interactions with other polar residues to pick up hydrogen bond interactions would enhance the potency of inhibitors. However, other isoenzymes also have the glucose-binding domain, which could cause selectivity issues when targeting HK2.

By contrast, targeting G6P binding could be a promising approach. Our docking studies revealed that G6P can interact with the helix-a5 catalytic domain and the linker helix-a13 domain, which are responsible for maintaining the unique catalytic function of the N-terminal domain specifically in HK2. These polar interactions, together with the additional polar interactions with ASP447, SER449, and LYS451 in the linker helix-a13, could be used to guide the optimization of the potency and selectivity of inhibitors. Moreover, we identified key fragments that are likely to bind to the G6P-binding site, such as

sulfonamido, polyhydroxypyran, lactam heterocycle, polycyclic ring, and multipolar groups. Lipophilic fragments, such as phenyl or cycloalkyl, are useful to reduce the polarity of the molecule, which could improve its permeability and, hence, bioavailability. These active fragments and their bioisosteres could be useful for the design of G6P mimics for targeting HK2.

A crystal structure of the HK2–VDAC1 complex is not yet available. For now, *in silico* modeling based on homology models might be a way forward to design inhibitors targeting the HK2–VDAC1 complex. We constructed a homology model of the HK2–VDAC1 complex for this purpose. The key interactions responsible for ligand binding were identified, which were specifically around the N-terminal helix of VDAC1 and the H anchor of the N terminus of HK2. We envisage that this information would be useful to rationalize the molecular interactions involved and aid the *in silico* design of inhibitors targeting the HK2–VDAC1 complex.

Currently, HK2 inhibitors designed through *in silico* models mainly target the glucose- and G6P-binding sites. Other HK2 inhibitors were identified via high throughput screening without follow-up elucidation of the binding modes to the target. However, many reported HK2 inhibitors were derived from natural products, suggesting virtual screening of natural product databases against HK2 as a promising direction to find novel hits. To enhance the chance of success in designing potent HK2 inhibitors, it would be helpful to incorporate fragments and their bioisosteres that are likely to interact with the binding pockets. Although various HK2 inhibitors against cancer have been developed, only few took full advantage of the structural information of the binding pocket in their molecular design. Given the important roles of HK2 in modulating cancer metabolism,<sup>68</sup> the discovery of potent and selective HK2 inhibitors using structure-based molecular design for anticancer treatment is likely to flourish in the years to come.

### Acknowledgements

We acknowledge financial support from the Science and Technology Development Fund, Macau SAR (File no. 0057/2018/A2) and University of Macau (File no. MYRG2019-00034-FHS). Helpful discussion and advice from Yizhen Guo are also gratefully acknowledged.

### References

- [1] M.G. Vander Heiden, L.C. Cantley, C.B. Thompson, Understanding the Warburg effect: the metabolic requirements of cell proliferation, *Science* 324 (5930) (2009) 1029–1033.
- [2] P. Warburg, On the origin of cancer cells, *Science* 123 (3191) (1956) 309–314.
- [3] O. Warburg, On the origin of cancer cells, *Science* 123 (3191) (1956) 309–314.
- [4] R.J. DeBerardinis, N.S. Chandel, Fundamentals of cancer metabolism, *Sci Adv* 2 (5) (2016) e1600200.
- [5] Z.E. Stine, Z.T. Schug, J.M. Salvino, C.V. Dang, Targeting cancer metabolism in the era of precision oncology, *Nat Rev Drug Discov* 21 (2) (2022) 141–162.
- [6] K.C. Patra, N. Hay, The pentose phosphate pathway and cancer, *Trends Biochem Sci* 39 (8) (2014) 347–354.
- [7] D. DeWaal, V. Nogueira, A.R. Terry, K.C. Patra, S.M. Jeon, G. Guzman, et al., Hexokinase-2 depletion inhibits glycolysis and induces oxidative phosphorylation in hepatocellular carcinoma and sensitizes to metformin, *Nat Commun* 9 (1) (2018) 446.
- [8] D.M. Irwin, H. Tan, Molecular evolution of the vertebrate hexokinase gene family: Identification of a conserved fifth vertebrate hexokinase gene, *Comp Biochem Phys D* 3 (1) (2008) 96–107.
- [9] H. Ardehali, Y. Yano, R.L. Printz, S. Koch, R.R. Whitesell, J.M. May, et al., Functional organization of mammalian hexokinase II. Retention of catalytic and regulatory functions in both the NH<sub>2</sub>- and COOH-terminal halves, *J Biol Chem* 271 (4) (1996) 1849–1852.
- [10] H. Ardehali, R.L. Printz, R.R. Whitesell, J.M. May, D.K. Granner, Functional interaction between the N- and C-terminal halves of human hexokinase II, *J Biol Chem* 274 (23) (1999) 15986–15989.
- [11] J.E. Wilson, Isozymes of mammalian hexokinase: structure, subcellular localization and metabolic function, *J Exp Biol* 206 (Pt 12) (2003) 2049–2057.
- [12] M.G. Hayes, M. Urbanek, M.F. Hivert, L.L. Armstrong, J. Morrison, C. Guo, et al., Identification of HKDC1 and BACE2 as genes influencing glycaemic traits during

- pregnancy through genome-wide association studies, *Diabetes* 62 (9) (2013) 3282–3291.
- [13] M.L. Cardenas, A. Cornish-Bowden, T. Ureta, Evolution and regulatory role of the hexokinases, *Biochim Biophys Acta* 1401 (3) (1998) 242–264.
- [14] T. Ureta, The comparative isozymology of vertebrate hexokinases, *Comp Biochem Phys B* 71 (4) (1982) 549–555.
- [15] R.A. Gatenby, R.J. Gillies, Why do cancers have high aerobic glycolysis?, *Nat Rev Cancer* 4 (11) (2004) 891–899.
- [16] S.P. Mathupala, Y.H. Ko, P.L. Pedersen, Hexokinase-2 bound to mitochondria: cancer's stygian link to the 'Warburg Effect' and a pivotal target for effective therapy, *Semin Cancer Biol* 19 (1) (2009) 17–24.
- [17] K.C. Patra, Q. Wang, P.T. Bhaskar, L. Miller, Z. Wang, W. Wheaton, et al., Hexokinase 2 is required for tumor initiation and maintenance and its systemic deletion is therapeutic in mouse models of cancer, *Cancer Cell* 24 (2) (2013) 213–228.
- [18] M. Anderson, R. Marayati, R. Moffitt, J.J. Yeh, Hexokinase 2 promotes tumor growth and metastasis by regulating lactate production in pancreatic cancer, *Oncotarget* 8 (34) (2017) 56081–56094.
- [19] R. Benz, Permeation of hydrophilic solutes through mitochondrial outer membranes - review on mitochondrial porins, *BBA-Rev Biomembranes* 1197 (2) (1994) 167–196.
- [20] V. De Pinto, F. Guarino, A. Guarnera, A. Messina, S. Reina, F.M. Tomasello, et al., Characterization of human VDAC isoforms: a peculiar function for VDAC3?, *Biochim Biophys Acta* 1797 (6–7) (2010) 1268–1275.
- [21] J.G. Pastorino, J.B. Hoek, Hexokinase II: the integration of energy metabolism and control of apoptosis, *Curr Med Chem* 10 (16) (2003) 1535–1551.
- [22] J.G. Pastorino, N. Shulga, J.B. Hoek, Mitochondrial binding of hexokinase II inhibits Bax-induced cytochrome c release and apoptosis, *J Biol Chem* 277 (9) (2002) 7610–7618.
- [23] N. Shulga, J.G. Pastorino, Hexokinase II binding to mitochondria is necessary for Kupffer cell activation and is potentiated by ethanol exposure, *J Biol Chem* 291 (24) (2016) 12574.
- [24] J.G. Pastorino, J.B. Hoek, Regulation of hexokinase binding to VDAC, *J Bioenerg Biomembr* 40 (3) (2008) 171–182.
- [25] H. Lin, J. Zeng, R. Xie, M.J. Schulz, R. Tedesco, J. Qu, et al., Discovery of a novel 2,6-disubstituted glucosamine series of potent and selective hexokinase 2 inhibitors, *ACS Med Chem Lett* 7 (3) (2016) 217–222.
- [26] W. Li, M. Zheng, S. Wu, S. Gao, M. Yang, Z. Li, et al., Benserazide, a dopadecarboxylase inhibitor, suppresses tumor growth by targeting hexokinase 2, *J Exp Clin Cancer Res* 36 (1) (2017) 58.
- [27] M. Zheng, C. Wu, K. Yang, Y. Yang, Y. Liu, S. Gao, et al., Novel selective hexokinase 2 inhibitor benitrobenzazide blocks cancer cells growth by targeting glycolysis, *Pharmacol Res* 164 (Feb 2021) 105367.
- [28] Liu HX. Lanzhou University. Human hexokinase 2 small molecule inhibitor and application thereof. CN112891342A.
- [29] M.H. Nawaz, J.C. Ferreira, L. Nedyalkova, H. Zhu, C. Carrasco-López, S. Kirmizialtin, et al., The catalytic inactivation of the N-half of human hexokinase 2 and structural and biochemical characterization of its mitochondrial conformation, *Biosci Rep* 38 (1) (2018). BSR20171666.
- [30] A.E. Aleshin, C. Zeng, H.D. Bartunik, H.J. Fromm, R.B. Honzatko, Regulation of hexokinase I: crystal structure of recombinant human brain hexokinase complexed with glucose and phosphate, *J Mol Biol* 282 (2) (1998) 345–357.
- [31] A.M. Mulichak, J.E. Wilson, K. Padmanabhan, R.M. Garavito, The structure of mammalian hexokinase-I, *Nat Struct Biol* 5 (7) (1998) 555–560.
- [32] J.C. Ferreira, A.R. Khrbtli, C.L. Shetler, S. Mansoor, L. Ali, O. Sensoy, et al., Linker residues regulate the activity and stability of hexokinase 2, a promising anticancer target, *J Biol Chem* 296 (2021) 100071.
- [33] S.N. Garcia, R.C. Guedes, M.M. Marques, Unlocking the potential of HK2 in cancer metabolism and therapeutics, *Curr Med Chem* 26 (41) (2019) 7285–7322.
- [34] H. Pelicano, D.S. Martin, R.H. Xu, P. Huang, Glycolysis inhibition for anticancer treatment, *Oncogene* 25 (34) (2006) 4633–4646.
- [35] C.L. Neary, J.G. Pastorino, Nucleocytoplasmic shuttling of hexokinase II in a cancer cell, *Biochem Biophys Res Commun* 394 (4) (2010) 1075–1081.
- [36] L.E. Raez, K. Papadopoulos, A.D. Ricart, E.G. Chiorean, R.S. Dipaola, M.N. Stein, et al., A phase I dose-escalation trial of 2-deoxy-D-glucose alone or combined with docetaxel in patients with advanced solid tumors, *Cancer Chemother Pharmacol* 71 (2) (2013) 523–530.
- [37] C. Marini, B. Salani, M. Massollo, A. Amaro, A.I. Esposito, A.M. Orengo, et al., Direct inhibition of hexokinase activity by metformin at least partially impairs glucose metabolism and tumor growth in experimental breast cancer, *Cell Cycle* 12 (22) (2013) 3490–3499.
- [38] G. Miao, J. Han, J. Zhang, Y. Wu, G. Tong, Targeting pyruvate kinase M2 and hexokinase II, pachymic acid impairs glucose metabolism and induces mitochondrial apoptosis, *Biol Pharm Bull* 42 (1) (2019) 123–129.
- [39] S.H. Jiang, F.Y. Dong, L.T. Da, X.M. Yang, X.X. Wang, J.Y. Weng, et al., Ikarugamycin inhibits pancreatic cancer cell glycolysis by targeting hexokinase 2, *FASEB J* 34 (3) (2020) 3943–3955.
- [40] F. Bao, K. Yang, C. Wu, et al., New natural inhibitors of hexokinase 2 (HK2): Steroids from *Ganoderma sinense*, *Article Fitoterapia ar* 125 (2018) 123–129.
- [41] A. Ehsani-Zonouz, A. Golestani, M. Nemat-Gorgani, Interaction of hexokinase with the outer mitochondrial membrane and a hydrophobic matrix, *Mol Cell Biochem* 223 (1–2) (2001) 81–87.
- [42] N. Haloi, P.C. Wen, Q. Cheng, M. Yang, G. Natarajan, A.K.S. Camara, et al., Structural basis of complex formation between mitochondrial anion channel VDAC1 and Hexokinase-II, *Commun Biol* 4 (1) (2021) 667.
- [43] B.D. Gelb, V. Adams, S.N. Jones, L.D. Griffin, G.R. MacGregor, E.R. McCabe, Targeting of hexokinase 1 to liver and hepatoma mitochondria, *Proc Natl Acad Sci U S A* 89 (1) (1992) 202–206.
- [44] P.G. Polakis, J.E. Wilson, An intact hydrophobic N-terminal sequence is critical for binding of rat-brain hexokinase to mitochondria, *Arch Biochem Biophys* 236 (1) (1985) 328–337.
- [45] F. Chiara, D. Castellaro, O. Marin, V. Petronilli, W.S. Brusilow, M. Juhaszova, et al., Hexokinase II detachment from mitochondria triggers apoptosis through the permeability transition pore independent of voltage-dependent anion channels, *PLoS ONE* 3 (3) (2008) e1852.
- [46] K.M. Smeele, R. Southworth, R. Wu, et al., Disruption of hexokinase II-mitochondrial binding blocks ischemic preconditioning and causes rapid cardiac necrosis, *Circ Res* 108 (10) (2011) 1165–1169.
- [47] D. Zhang, Y.M. Yip, L. Li, In silico construction of HK2-VDAC1 complex and investigating the HK2 binding-induced molecular gating mechanism of VDAC1, *Mitochondrion* 30 (2016) 222–228.
- [48] Z. Chen, H. Zhang, W. Lu, P. Huang, Role of mitochondria-associated hexokinase II in cancer cell death induced by 3-bromopyruvate, *Biochim Biophys Acta* 1787 (5) (2009) 553–560.
- [49] D. Xu, J. Jin, H. Yu, Z. Zhao, D. Ma, C. Zhang, et al., Chrysin inhibited tumor glycolysis and induced apoptosis in hepatocellular carcinoma by targeting hexokinase-2, *J Exp Clin Cancer Res* 36 (1) (Mar 20 2017); 44.
- [50] Tidmarsh G. Threshold Pharmaceuticals, Inc. Combination therapies for the treatment of cancer. patent US20060276527A1; patent application PCT/US04/01138.
- [51] L. Zhou, M. Li, X. Yu, F. Gao, W. Li, Repression of hexokinases II-mediated glycolysis contributes to piperlongumine-induced tumor suppression in non-small cell lung cancer cells, *Int J Biol Sci* 15 (4) (2019) 826–837.
- [52] Behar V, Becker OM, Pahima HT, Yosef HR. VIDAC Pharma Ltd. Use of hexokinase 2/mitochondria-detaching compounds for treating hexokinase-2 (HK2)-expressing cancers. patent WO2018083705A1; patent application PCT/IL2017/051214.
- [53] V. Behar, H. Pahima, A. Kozminsky-Atias, N. Arbel, E. Loeb, M. Herzberg, et al., A hexokinase 2 modulator for field-directed treatment of experimental actinic keratoses, *J Invest Dermatol* 138 (12) (2018) 2635–2643.
- [54] J.K. Fraser, F.K. Lin, M.V. Berridge, Expression and modulation of specific, high affinity binding sites for erythropoietin on the human erythroleukemic cell line K562, *Blood* 71 (1) (1988) 104–109.
- [55] P. Pasdois, J.E. Parker, A.P. Halestrap, Extent of mitochondrial hexokinase II dissociation during ischemia correlates with mitochondrial cytochrome c release, reactive oxygen species production, and infarct size on reperfusion, *J Am Heart Assoc* 2 (1) (2012) e005645.
- [56] H. Li, S. Hu, Y. Pang, M. Li, L. Chen, F. Liu, et al., Bufalin inhibits glycolysis-induced cell growth and proliferation through the suppression of Integrin beta2/FAK signaling pathway in ovarian cancer, *Am J Cancer Res* 8 (7) (2018) 1288–1296.
- [57] Y. Yang, Y. Cao, L. Chen, F. Liu, Z. Qi, X. Cheng, et al., Cryptotanshinone suppresses cell proliferation and glucose metabolism via STAT3/SIRT3 signaling pathway in ovarian cancer cells, *Cancer Med* 7 (9) (2018) 4610–4618.
- [58] Y.P. Huang, N.W. Chang, Proteomic analysis of oral cancer reveals new potential therapeutic targets involved in the Warburg effect, *Clin Exp Pharmacol Physiol* 44 (8) (2017) 880–887.
- [59] G.Q. Chen, C.F. Tang, X.K. Shi, C.Y. Lin, S. Fatima, X.H. Pan, et al., Halofuginone inhibits colorectal cancer growth through suppression of Akt/mTORC1 signaling and glucose metabolism, *Oncotarget* 6 (27) (2015) 24148–24162.

- [60] J. Wu, X. Zhang, Y. Wang, Q. Sun, M. Chen, S. Liu, et al., Licochalcone A suppresses hexokinase 2-mediated tumor glycolysis in gastric cancer via downregulation of the Akt signaling pathway, *Oncol Rep* 39 (3) (2018) 1181–1190.
- [61] X. Gao, H. Han, Jolkinolide B inhibits glycolysis by downregulating hexokinase 2 expression through inactivating the Akt/mTOR pathway in non-small cell lung cancer cells, *J Cell Biochem* 119 (6) (2018) 4967–4974.
- [62] S. Agnihotri, S. Mansouri, K. Burrell, M. Li, Y. Mamatjan, J. Liu, et al., Ketoconazole and posaconazole selectively target HK2-expressing glioblastoma cells, *Clin Cancer Res* 25 (2) (2019) 844–855.
- [63] Z. Li, X. Tang, Y. Luo, B. Chen, C. Zhou, X. Wu, et al., NK007 helps in mitigating paclitaxel resistance through p38MAPK activation and HK2 degradation in ovarian cancer, *J Cell Physiol* 234 (9) (2019) 16178–16190.
- [64] Z. Lu, Y. Guo, X. Zhang, J. Li, L. Li, S. Zhang, et al., ORY-1001 suppresses cell growth and induces apoptosis in lung cancer through triggering HK2 mediated warburg effect, *Front Pharmacol* 9 (2018) 1411.
- [65] W. Dai, F. Wang, J. Lu, Y. Xia, L. He, K. Chen, et al., By reducing hexokinase 2, resveratrol induces apoptosis in HCC cells addicted to aerobic glycolysis and inhibits tumor growth in mice, *Oncotarget* 6 (15) (2015) 13703–13717.
- [66] Q. Zhang, Q. Liu, S. Zheng, T. Liu, L. Yang, X. Han, et al., Shikonin inhibits tumor growth of ESCC by suppressing PKM2 mediated aerobic glycolysis and STAT3 phosphorylation, *J Cancer* 12 (16) (2021) 4830–4840.
- [67] Y. Zhou, X. Zheng, J. Lu, W. Chen, X. Li, L. Zhao, Ginsenoside 20(S)-Rg3 inhibits the Warburg effect via modulating DNMT3A/ MiR-532-3p/HK2 pathway in ovarian cancer cells, *Cell Physiol Biochem* 45 (6) (2018) 2548–2559.
- [68] Y. Zhou, Y. Guo, K.Y. Tam, Targeting glucose metabolism to develop anticancer treatments and therapeutic patents, *Expert Opin Ther Pat* 32 (4) (2022) 441–453.